ACS APPLIED BIO MATERIALS

www.acsabm.org Article

Use of Target-Specific Liposome and Magnetic Nanoparticle Conjugation for the Amplified Detection of Norovirus

Ankan Dutta Chowdhury,[#] Sabrina Sharmin,[#] Fahmida Nasrin, Masahito Yamazaki, Fuyuki Abe, Tetsuro Suzuki, and Enoch Y. Park*

Cite This: *ACS Appl. Bio Mater.* 2020, 3, 3560−3568 Read Online

ACCESS | Metrics & More | Article Recommendations | Supporting Information

ABSTRACT: Viral diseases are one of the most life-threatening diseases as they can erupt unpredictably and spread rapidly in any medium with a very small number of particles. Therefore, the key for lethal virus detection should be highly sensitive in the early-stage detection, which can help increase the chance of survival. Amplification of the detecting signal is one of the most promising mechanisms for the detection of low-concentration analytes. A proper amplification can develop such a kind of system where a small number of particles can produce intense signals for a prominent detection. Keeping this in mind, in this report, we have presented a fluorometric method to detect norovirus (NoV) by a newly developed fluorophore-labeled liposome and a magnetically modified Fe_3O_4 combined system. Homogeneously distributed amine-functionalized liposomes have been constructed filled with a strong fluorophore of calcein. Simultaneously, (3-aminopropyl)-triethoxysilane (APTES)-functionalized Fe_3O_4 nanoparticles are also synthesized by the standard silanization process, and these two separately synthesized nanoparticles were functionalized with an antibody to achieve specificity. The Fe_3O_4 and calcein−liposome system has been applied for NoV detection, which was magnetically separated from the analyte medium and then externally burst to release the fluorophores from the core of the liposome. The easiness, rapidity, and sensitivity in a wide linear range can offer a huge potential of this method in point-of-care diagnostics.

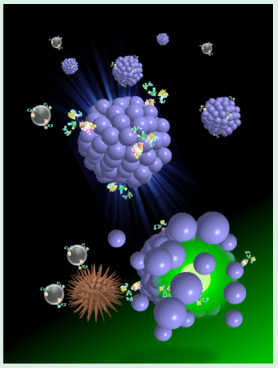

KEYWORDS: *liposomes, calcein, confocal, virus, biosensor, fluorescence*

INTRODUCTION

The recent ongoing growth of nanotechnology in science offers new prospects for the development of ultrasensitive detection tools that can be applied to detect extremely low level of analytes, amplifying the sensing outputs.[1−11] The ability to detect very small number of analytes remains an indefinable area with broad implications in various biomedical diagnostics at a very early stage of viral infection.[12−14] The current methods on virus detection mostly rely on sample enrichment through cell culture or nucleic acid-based tests or various established virus detection approaches like enzyme-linked immunosorbent assay (ELISA),[15] polymerase chain reaction (PCR),[16] virus isolation, and next-generation sequencing.[17,18] However, in spite of their limited available diagnostic assays, these are highly expensive, time-consuming, and need specialized personnel to operate.[18−20]

Therefore, a reliable biosensor is in great demand to overcome the emerging outbreak by early detection of the disease agent, where the key requirement is to determine the occurrence of a virus in the sample, irrespective of its concentration.[6,21] Therefore, the sensor can be designed in such a way that it can offer a maximum response of the target analyte down to a single or few pathogens, amplifying the sensing outputs.[21−23] To achieve this, liposomes are an attractive approach owing to their versatile and unique properties for the application in the field of biosensing.[24−27] They are also known for amplification where a single pathogen attached with a single liposome can produce multiple signals, releasing their encapsulated signaling probes.[26] Therefore, a small number of analytes can produce very large number of intense signals, which can be detected by the detector. Another advantage of liposome-based systems is that the encapsulated probes remain protected and almost inactive inside the liposome, which can reduce the background noise significantly.[28]

Encouraged by our previous reports on liposomal amplification,[26] in this study, a fluorophore of calcein-encapsulated 1-palmitoyl-2-oleoyl-*sn*-glycero-3-phosphocholine:1,2-dioleoyl-*sn*-glycero-3-phospho-(1′-rac-glycerol):1,2-distearoyl-*sn*-glycero-3-phosphoethanolamine-*N*-[amino(polyethylene glycol)-2000] (DOPC/DOPG/DSPE-PEG_{2000}) amine liposomes has been synthesized, which can be used for the detection of virus where DOPC and DOPG are the main liposomal content and DSPE-PEG_{2000} amine has been used to achieve amine functionalization.[29] As the main goal of this present work is to achieve detectability at very low levels of virus concentration, the

Received: February 26, 2020
Accepted: April 22, 2020
Published: April 22, 2020

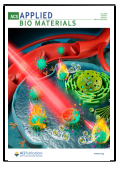

https://dx.doi.org/10.1021/acsabm.0c00213
ACS Appl. Bio Mater. 2020, 3, 3560−3568

purification of the target virus from the medium should be extremely important, especially for the real-sample analysis.[30] To serve this purpose, the well-established amine-functionalized Fe_3O_4 magnetic nanoparticles have been used, synthesized by the standard silanization process.[31] To make the liposomes as well as Fe_3O_4 nanoparticles specific toward the target virus, which is the norovirus (NoV) chosen as a model, the corresponding antibody has been conjugated by the succinimidyl 4-(*N*-maleimidomethyl)cyclohexane-1-carboxylate (SMCC) and *N*-(3-(dimethylamino)-propyl)-*N*′-ethylcarbodiimide hydrochloride/*N*-Hydroxysuccinimide (EDC/NHS) covalent binding approach through their functionalized amine group. On adding different concentrations of viruses in this sensing system, calcein−liposome and magnetic Fe_3O_4 nanoparticles can bind to the viruses and form a sandwich-like structure. The Fe_3O_4-conjugated calcein−liposome system magnetically separates from its analyte medium and then lyses out the fluorophores from the core of the liposome using Triton X as a surfactant. Hence, a large number of fluorophores can come out from a small number of virus-captured calcein−liposome nanoconjugates and amplify the detection signal significantly. The optimizing conditions for sensor formulation and its sensing parameters are investigated thoroughly. The detection limit has been found in the range of hundred copies per mL of viruses. The minimal cross-reactivity with similar viruses and stability test for a month confirms the formation of nonleaky and specific liposomal sensors with low background noise and high specificity toward the targeted virus. Consequently, an efficient signal amplification can be achieved, which met the requirements of its potential usage for real-sample monitoring.

MATERIALS AND METHODS

Chemicals. 1-Palmitoyl-2-oleoyl-*sn*-glycero-3-phosphocholine (DOPC), 1,2-dioleoyl-*sn*-glycero-3-phospho-(1′-rac-glycerol) (DOPG) and 1,2-distearoyl-*sn*-glycero-3-phosphoethanolamine-*N*-[amino(polyethylene glycol)-2000] (ammonium salt) (DSPE-PEG_{2000} amine) were purchased from Avanti Polar Lipids (Alabaster, AL). Sodium citrate, $FeCl_3{\cdot}6H_2O$, and $FeCl_2{\cdot}4H_2O$ were obtained from Wako Pure Chemical Industries Ltd. (Japan). Ammonia solution (28% (w/v)), (3-aminopropyl)-triethoxysilane (APTES), *N*-(3-(dimethylamino)-propyl)-*N*′-ethylcarbodiimide hydrochloride (EDC), *N*-hydroxysuccinimide (NHS), and dry toluene were purchased from Sigma-Aldrich (St. Louis). Analytical grade of toluene and other solvents were used as received without any further purification. Succinimidyl 4-(*N*-maleimidomethyl)cyclohexane-1-carboxylate (SMCC) was purchased from Thermo Fisher (Tokyo, Japan). Anti-NoV monoclonal antibody (NS14) that recognizes the C-terminal P1 subdomain of the capsid protein of NoV genogroup II obtained from the spleen cells of mice immunized orally was utilized here.[32] The obtained antibody was purified by protein G, and the stock concentration was 0.3 mg mL^{-1}.[33,34] All of the solutions were prepared in deionized water (18.2 MΩ cm) unless otherwise mentioned through a UV-treated RephiLe water system.

Preparation of Fe_3O_4 Nanoparticles. The synthesis of Fe_3O_4 nanoparticles was carried out through the standard procedure, as described previously.[35] The magnetic samples were washed repeatedly and separated by magnetic separation.

Functionalization of Fe_3O_4 Nanoparticles. The as-synthesized Fe_3O_4 nanoparticles were coated with APTES using the standard method of silanization.[36] In brief, APTES was first dissolved in dry toluene and then the dried Fe_3O_4 nanoparticles were added to it in an inert atmosphere. The mixture was then refluxed at 120 °C for 20 h under constant stirring. After successful formation, the APTES-coated Fe_3O_4 was washed with fresh toluene to discard the excess APTES. Finally, the product was dried overnight and kept for further use. For the purpose of sensing, 1 mg of Fe_3O_4 nanoparticles was dispersed in 1 mL of phosphate-buffered saline (PBS) to prepare the 1 mg mL^{-1} concentration, which was used throughout all experiments. An approximate particle number of the Fe_3O_4 nanoparticles is estimated in **S5** of the Supporting Information.

Preparation of Different Types of Liposome. DOPC/DOPG/DSPE-PEG_{2000} amine liposomes (molar ratios: 30:50:20, 35:50:15, 40:50:10, and 45:50:5) were prepared using the natural swelling method in a buffer at 37 °C, and then the liposomes were prepared according to our previous work.[37] Initially, all of the phospholipids were prepared in a 7.4 pH PBS solution at a 1 mM stock concentration. Then, a total volume of 200 μL of the phospholipids mixture was taken for the lipid film formation. For example, in the case of 30:50:20 molar ratio liposome, 60 μL of DOPC, 100 μL of DOPG, and 40 μL of DSPE-PEG_{2000} amine were mixed. After that, 1 mL of different concentrations of calcein containing PBS was added to hydrate the film for the preparation of calcein−liposome. Finally, the liposomes were purified by the membrane filtering method using a 0.8 μm polycarbonate membrane (Merck, Carrigtwohill, Ireland). The concentration of the liposomes has been calculated in the range of 10^{12} particles mL^{-1} by the number-concentration based on lipids' volume (VOL method),[38] as described in **S5** of the Supporting Information.

Antibody Conjugation with Fe_3O_4 Nanoparticles and Liposome Separately. The same monoclonal anti-NoV antibody was conjugated on the APTES-coated Fe_3O_4 and liposome separately according to the following protocol.[39] Initially, 1 mg of APTES-coated Fe_3O_4 in 1 mL of PBS and 1 mL of the as-prepared liposome were conjugated with 6 mg of sulfo-SMCC. The antibody was conjugated with 180 μL of iminothiolane and incubated for 1 h at room temperature. Then, the liposome and Fe_3O_4 nanoparticles were mixed with the iminothiolane-conjugated antibody. The reaction mixture was incubated for 30 min at room temperature to obtain the final product.[40] Then, the antibody-conjugated liposomes and Fe_3O_4 were dialyzed in a 1 kDa dialysis bag for 24 h (dialysate was replaced every 8 h) to remove the excess antibody.

Detection of Clinically Isolated NoV. Clinically isolated GII NoV were collected from the fecal samples of the patients with infection by inspections based on laws and ordinances. The sampling of Norovirus was carried out according to the proper guideline, after getting approval from the Ethics Committee of Environment and Hygiene Institute in Shizuoka Prefecture (September 14, 2016). The fecal sample (100 μg) was added to 900 μL of phosphate-buffered saline (PBS, pH 7.4), solids were separated, and the supernatant was used for the detection. The concentration of GII NoV in the supernatant was evaluated to be 6.2×10^7 copies mL^{-1} by real-time PCR.[41] For further study, serial dilutions were made from this stock solution. For the selectivity test, influenza virus A (Avian/Vietnam/1203/04) (H5N1) (lot: GR301823−1) was purchased from Abcam, Inc. (Cambridge, UK). Zika virus- (PRVABC-59) and hepatitis E virus-like particles (HEV-LP) were kindly provided by Professor K. Morita of Institute of Tropical Medicine, Nagasaki University.

The calcein−liposome solution (100 μL) was mixed with 20 μL of 1 mg mL Fe_3O_4 nanoparticles at different concentrations of 80 μL of NoV and incubated for 10 min in different reaction chambers. Then, an external magnet of 20 T was placed at the bottom of each chamber for 5 min to separate the calcein−liposome/NoV/Fe_3O_4 sandwich structure, discarding the excess reactants and other impurities. After the separation, the mixture was redispersed with 100 μL of fresh buffer in a microplate reader and 5 μL of a 0.1 mM Triton X solution was added to disrupt the liposome. The sample solution was excited at 450 nm, and the fluorescence intensity was measured in a range of 500−700 nm before and after Triton X addition. After receiving the collected virus sample for analysis, the formation of the calcein−liposome/NoV/Fe_3O_4 sandwich structure and its detection take approximately 20 min to obtain the result.

Characterizations. The transmission electron microscopy (TEM) images of the liposome, Fe_3O_4, and their nanocomposites were taken by JEOL TEM (JEOL, Tokyo, Japan). To obtain high-resolution images, HR-TEM (1400 JEM-2100F at 200 kV, JEOL, Tokyo, Japan) was used. UV−vis absorption and fluorescence spectra were measured using a

https://dx.doi.org/10.1021/acsabm.0c00213
ACS Appl. Bio Mater. 2020, 3, 3560−3568

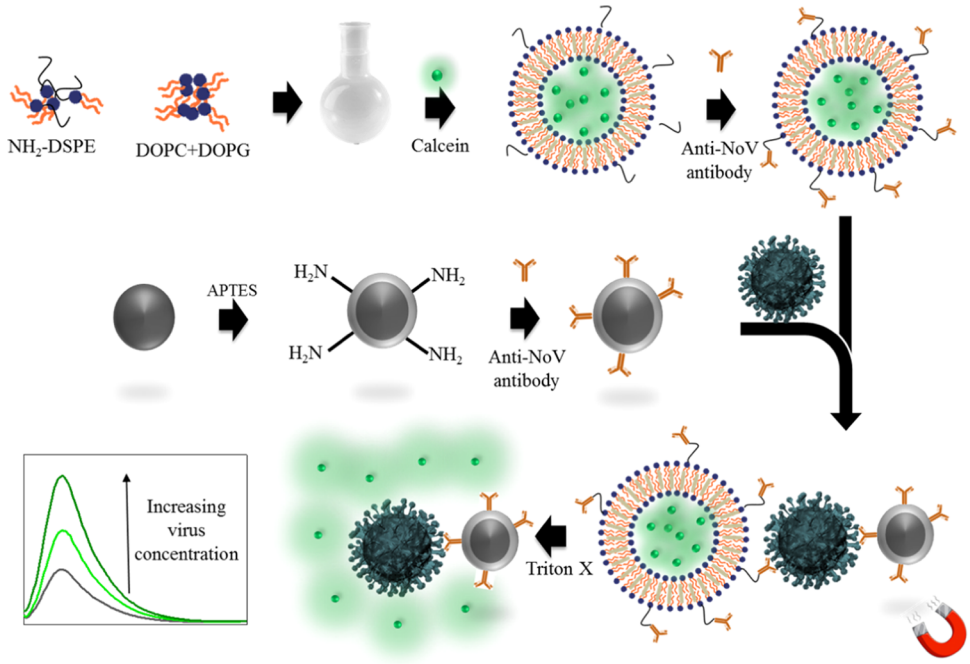

Figure 1. Schematic representation of the formation of calcein−liposome and Fe_3O_4 nanoparticles and the mechanism of the detection of NoV.

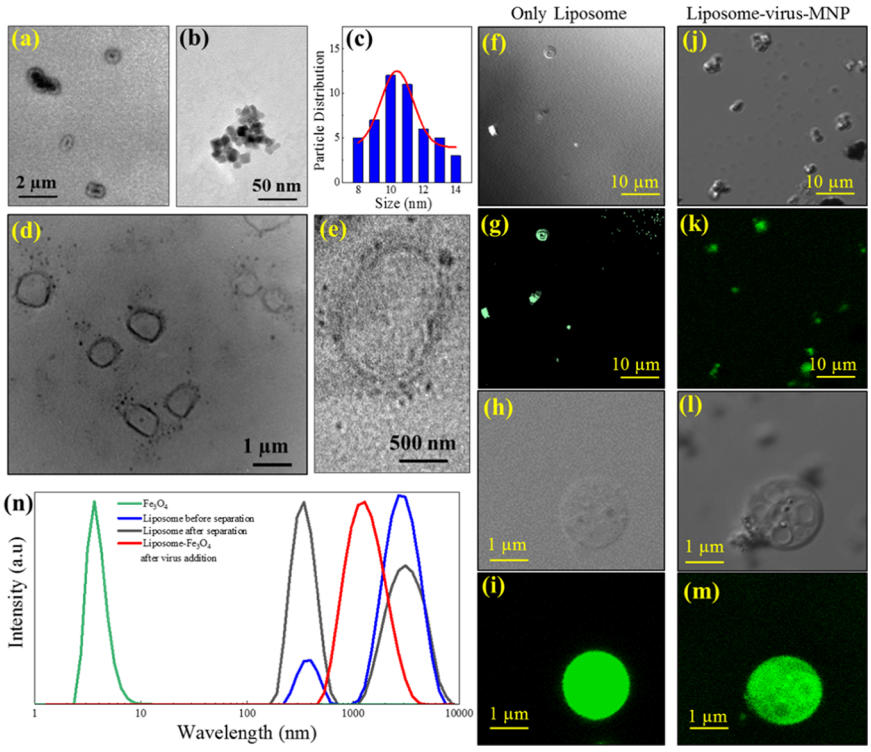

Figure 2. Characterizations of individually synthesized calcein−liposome, Fe_3O_4 nanoparticles, and calcein−liposome/virus/Fe_3O_4 nanoconjugates: (a) bare liposomes, (b) bare Fe_3O_4 nanoparticles and (c) their size distribution, and (d) HRTEM image of calcein−liposome/virus/Fe_3O_4 nanoconjugates and (e) their magnified image. Differential interference contrast (DIC) and fluorescence images in a confocal microscope for (f−i) only calcein−liposomes and (j−m) calcein−liposome/virus/Fe_3O_4 nanoconjugates. (n) Hydrodynamic radius of the as-synthesized liposome, Fe_3O_4 nanoparticles, and calcein−liposome/virus/Fe_3O_4 nanoconjugates.

filter-based multimode microplate reader (Infinite F500; TECAN Ltd., Männedorf, Switzerland). Dynamic light scattering (DLS) was carried out using a Zetasizer Nano series (Malvern Instruments Ltd., Malvern, UK). The images of liposomes were taken in a confocal laser scanning microscope (FV-1000, Olympus, Tokyo, Japan) using a stage thermocontrol system (ThermoPlate, Tokai Hit, Shizuoka, Japan).

RESULTS AND DISCUSSION

In this study, a highly sensitive fluorescence signal amplification-based strategy has been proposed for the detection of NoV using calcein−liposome and Fe_3O_4 nanoparticle conjugates. According to our hypothesis, in the presence of the target NoV,

https://dx.doi.org/10.1021/acsabm.0c00213
ACS Appl. Bio Mater. 2020, 3, 3560−3568

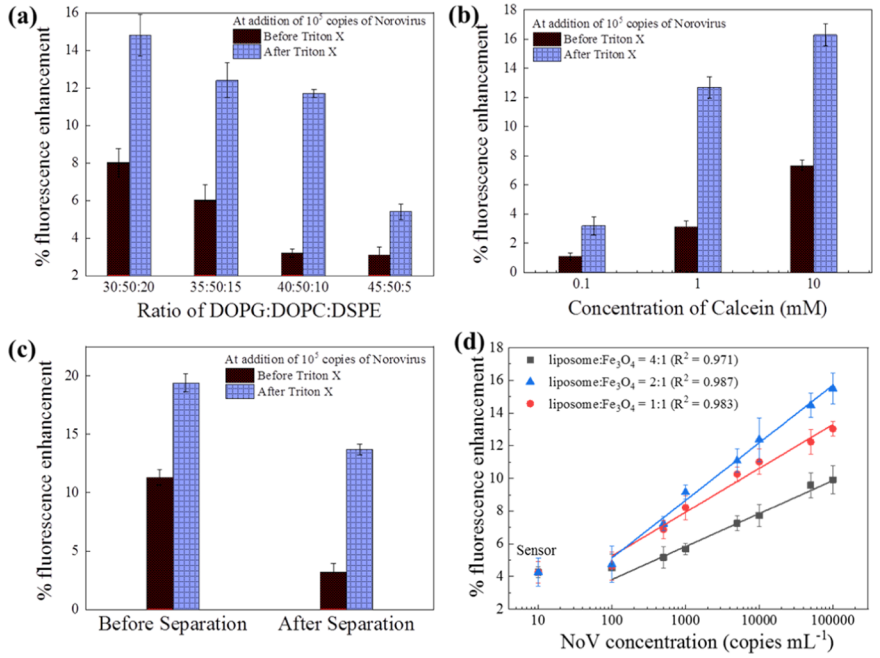

Figure 3. Optimization of calcein−liposome and Fe_3O_4 nanoconjugates for the detection of NoV. (a) Effect of DOPC, DOPG, and DSPE-PEG_{2000} amine ratios of 30:50:20, 30:50:15, 40:50:10, and 40:50:5 in the presence of 10^5 copies mL^{-1} NoV. (b) Effect of calcein dye loading concentrations of 0.1, 1, and 10 mM in the presence of 10^5 copies mL^{-1} NoV. (c) Effect of 0.8 μm size separation of calcein−liposome. (d) Calibration lines obtained from different calcein−liposome and Fe_3O_4 nanoparticles ratios at concentrations of 10^2−10^5 copies mL^{-1} NoV.

antibody-conjugated two nanoparticles should bind with the virus and can form a sandwich-like structure, as depicted in Figure 1. The calcein−liposome/NoV/Fe_3O_4 nanoconjugates then separate from the sample medium by the magnetic process, discarding mixing of other interfering compounds. Thereafter, the successful release of the encapsulated fluorophores by Triton X surfactant can estimate the amount of the viruses by indirect calibration. The advantage of the present study finds three important aspects, which can make the system a good alternative for the virus detection process: (i) Usage of liposomal platform can amplify the single virus signal to multiple fluorophores; (ii) due to the magnetic separation, the system can eliminate the interfering reagents of the sample, which is the key point for direct virus detection; and (iii) formation of the calcein−liposome/NoV/Fe_3O_4 rigid system by covalent bonding and thereafter specific antigen−antibody interaction reduces the background signal significantly, improving the detection sensitivity.

Liposome and Fe_3O_4 Nanoparticle Synthesis and Characterizations. Different compositions of phospholipids of DOPG, DOPC, and DSPE-PEG_{2000} amine have been used for the synthesis of liposomes, where the encapsulated calcein concentrations are also varied. To obtain size-specific liposomes, the as-synthesized liposomes were passed through a 0.8 μm polycarbonate membrane. Similarly, Fe_3O_4 nanoparticles were also synthesized via the sol−gel method and coated with APTES. For characterization, 100 μL of liposome (40:50:10 ratio of phospholipids) with 0.1 M encapsulated calcein and 20 μL of 0.1 mg mL^{-1} Fe_3O_4 nanoparticle was tested on 80 μL of 10^5 copies mL^{-1} NoV to form the calcein−liposome/virus/Fe_3O_4 nanoconjugates. These two nanoparticles are individually characterized by their TEM images presented in Figure 2a,b. The liposomes are formed in a homogeneously distributed circular form. The bare Fe_3O_4 nanoparticles are shown in the range of 8−14 nm of size with an average diameter of 10.5 nm (Figure 2c). In the presence of the virus, these two nanoparticles successfully form the calcein−liposome/virus/Fe_3O_4 nanoconjugates with the expected sandwich structure, as shown in the TEM image of Figure 2d. The small intense black dots of Fe_3O_4 situated in the outside of the liposomes structure was clearly shown in the TEM image. In the high-magnification image in Figure 2e, the nanoconjugate formation is more visible with a small but clear distance between them, indicating the presence of small-size virus particles. As the TEM grids are not stained to observe the morphology of the nanoparticles in a good manner, the virus is not recognizable in the TEM image. The structures were further characterized by their confocal images. The phase contrast image of only liposome in Figure 2f and the magnified image of a single liposome in Figure 2h show the perfectly spherical formation, which emits the intense green fluorescence of calcein in their fluorescence image at 520 nm (Figure 2g,i).[37] After the addition of virus, these two nanoparticles, conjugated with antibody, were formed as calcein−liposome/virus/Fe_3O_4 nanoconjugates. The antibody conjugation was tested by the standard ELISA method, as shown in Figure S1 of the Supporting Information. In the phase contrast images of calcein−liposome/virus/Fe_3O_4 nanoconjugates in Figure 2j,l, there are few dark spots clearly observed besides the liposomal structure, representing the structure of Fe_3O_4 nanoparticles. In the fluorescence images in Figure 2k,m, those dark spots do not emit any fluorescence signal as expected, eliminating any possibilities of aggregated lipids. As the spherical radius of the liposome and Fe_3O_4 is largely deviated, the images were not properly focused on both nanoparticles at a time.

The formation of calcein−liposome/virus/Fe_3O_4 nanoconjugates is also confirmed by their hydrodynamic radius found in DLS, as depicted in Figure 2n. The average size of the as-synthesized Fe_3O_4 and calcein−liposome was found to be 6 (PDI 0.3) and 2112 nm (PDI 0.27), respectively. The liposome size significantly showed a major contribution at 506.5 nm (PDI

https://dx.doi.org/10.1021/acsabm.0c00213
ACS Appl. Bio Mater. 2020, 3, 3560−3568

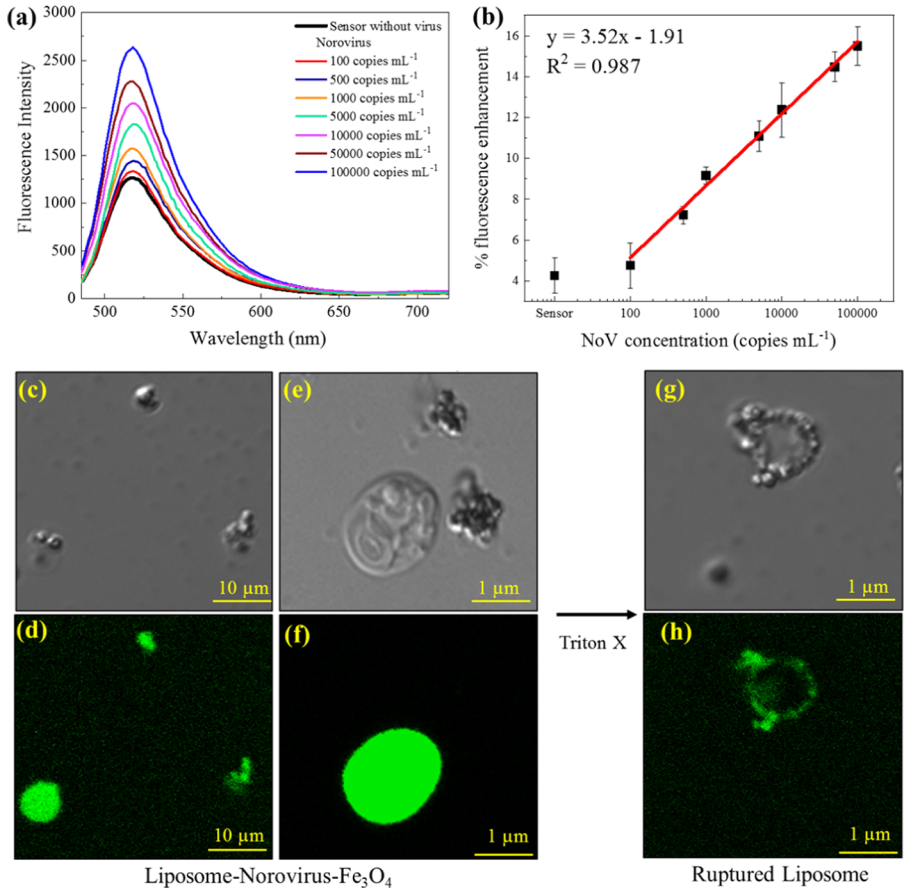

Figure 4. Detection of NoV. (a) Fluorescence of calcein, released from the calcein–liposome/NoV/Fe_3O_4 nanoconjugates with various NoV concentrations from 10^2–10^5 copies mL^{-1}, after treated with Triton X. (b) Calibration line of fluorescence peak intensities vs concentration of NoV. Confocal images of the liposome/NoV/Fe_3O_4 nanoconjugates with 10^5 copies mL^{-1} of NoV (c–f) before and (g,h) after addition of Triton X.

0.21) after the size neutralization, which confirms the uniformity. However, there is still some liposomal contribution at 2112 nm, which becomes less intense compared to the size-separated liposomes. After the formation of calcein–liposome/virus/Fe_3O_4 nanoconjugates, the size of the nanocojugates increased to 1120 nm, indicating the formation of the sandwich-like structure. Due to the conjugation of 40 nm NoV with several Fe_3O_4 nanoparticles, the agglomerated liposome/virus/Fe_3O_4 nanoconjugates show a large hydrodynamic diameter in DLS.

Fe_3O_4-Conjugated Calcein–Liposome Formulation and Its Optimized Condition for Virus Detection. Initially, the synthesis of a nonpermeable and stable liposome has been optimized with different concentrations of the lipids, varying their ratios. To investigate this condition, we have initially decided to take the ratio of DOPC and DOPG as 1:1, referring from the recent literature.[42,43] However, to achieve amine functionality, the DSPE-PEG_{2000} amine has also been introduced in lipids where the ratios were varied as 30:50:20, 35:50:15, 40:50:10, and 45:50:5. Initially, the production of nonleaky liposomes has been verified by the control experiment, as presented in Figure S2. All of the calcein-encapsulated liposomes were treated with Triton X, and their fluorescence has been compared to that of the untreated one. In all cases, the results confirm the formation of the nonleaky liposome. Then, the formation of calcein–liposome/virus/Fe_3O_4 nanoconjugates has been optimized for all types of liposomes with different lipid compositions using the standard concentration of NoV of 10^5 copies mL^{-1}. In the cases of 45:50:5 and 40:50:10, the background intensities after forming the conjugates without the treatment of Triton X are found to be extremely high compared to other compositions (Figure 3a). To achieve more amine functionalization, a higher DSPE-PEG_{2000} amine content should be more desirable. Therefore, the 40:50:10 composition has been selected for further studies, where the best results are obtained at the highest amine content. Next, to investigate the maximum loading concentration of the fluorophore dye, calcein, during the liposomal synthesis, three different concentrations of calcein (0.1, 1, and 10 mM) have been used for the encapsulation inside the best suited 40:50:10 liposome, and then the formation of the calcein–liposome/virus/Fe_3O_4 nanoconjugates was tested with NoV of 10^5 copies mL^{-1}. It is clear from Figure 3b that except 0.1 mM of calcein, the other two concentrations show significant fluorescence signals. As the concentration of the target virus should be low enough, it is highly desirable to load the maximum amount of dye inside the liposome for low-level detection. Therefore, the 0.1 mM concentration of calcein–liposome was rejected. Compared to the other two concentrated calcein-encapsulated liposomes, the overall fluorescence intensity of 1 mM is quite similar to the 10 mM concentration, however with low background signal. As the nonspecific binding shows a large interference in the highest concentration, the 1 mM concentration of the calcein–liposome was selected as the optimum for further studies. Beside the concentration of the encapsulated dye, the intensity of the fluorescence signal is highly dependent on the size of the liposome. To obtain a uniform result, the 0.8 μm pore-sized

https://dx.doi.org/10.1021/acsabm.0c00213
ACS Appl. Bio Mater. 2020, 3, 3560–3568

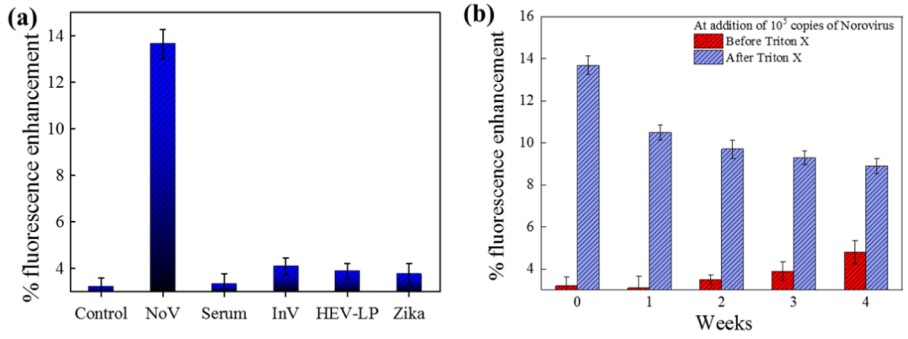

Figure 5. Specificity and stability of the calcein−liposome and Fe_3O_4 system. (a) Fluorometric enhancement of calcein−liposome and Fe_3O_4 system in the presence of the target NoV (10^5 copies mL^{-1}), 10-fold diluted human serum, H1N1 influenza virus (10^5 copies mL^{-1}), hepatitis E virus-like particles (10^9 g mL^{-1}), and zika virus (10^6 copies mL^{-1}). (b) Stability test of the calcein−liposome and Fe_3O_4 with 10^5 copies mL^{-1} of NoV before (red bars) and after (blue bars) addition of Triton X over a 4-week period.

polycarbonate membrane was applied to separate the as-mixed sized calcein−liposome to a uniformly distributed liposomal mixture, which was already characterized previously in the DLS section of Figure 2n. When the as-prepared and size-normalized calcein−liposomes are treated with NoV of 10^5 copies mL^{-1} and thereafter Triton X, the sensitivity has changed significantly (Figure 3c). Uniformly distributed liposomes of size 0.8 μm or less show much better signals compared to the background signal.

After optimizing the composition of the liposome and the concentration of the encapsulated calcein concentration, the formation of the calcein−liposome/virus/Fe_3O_4 nanoconjugates has been finally tested with different ratios of the magnetic Fe_3O_4 nanoparticles. In this process, the target virus has been bound with liposome and Fe_3O_4 in a sandwich-like structure and then isolated from the magnetic separation. Therefore, a larger number of Fe_3O_4 nanoparticles can enhance the possibility of better separation. However, on the other hand, a large number of Fe_3O_4 nanoparticles can attach to the virus particle itself without conjugation of the liposome, resulting in a false negative signal, whereas a small number of Fe_3O_4 nanoparticles could not attach all of the viruses along with the liposomes. Therefore, optimization of the Fe_3O_4 nanoparticles is a crucial parameter for this sandwich sensor, where the trend of the detection has been investigated in the concentration range of 10^2−10^5 copies mL^{-1} of NoV, varying with different ratios of liposomes and Fe_3O_4 nanoparticles (4:1, 2:1, and 1:1). The concentration of the Fe_3O_4 nanoparticles remains constant at 1 mg mL^{-1}, which is higher than the optimum for the binding with viruses even at a high concentration of 10^6 copies mL^{-1}, where the concentration of liposome was varied. As shown in Figure 3d, for all three cases, the sensor shows good linearity; however, the limit of detection, calculated by the $3\sigma/S$ method (three times of the standard deviation of the lowest concentration of target/slope of the calibration line), has been found to be 267, 136, and 150 copies mL^{-1}, respectively.[44] In terms of the detection limit and the R^2 value for linearity, the 2:1 ratio shows the best optimized condition for virus detection.

Detection of NoV by Fe_3O_4 and Calcein−Liposome and Its Structural Conformation in Confocal Images. Summarizing all optimizing parameters for calcein−liposome/virus/Fe_3O_4 nanoconjugates, it has applied for the detection of different concentrations of NoV, as presented in Figure 4a. Before virus addition, the reaction medium contains anti-NoV antibody-conjugated free calcein−liposome and Fe_3O_4 nanoparticles. There is no substantial interaction between these two, which was tested as a control experiment and is presented in Figure S3 of the Supporting Information. However, after the addition of 80 μL of virus on 100 μL of calcein−liposome and 20 μL of Fe_3O_4 nanoparticles for 10 min, the nanoparticles have been bound with viruses through the specific antibody on their surfaces. Therefore, the magnetically isolated calcein−liposome/virus/Fe_3O_4 nanoconjugates show an intense signal of the calcein after the disruption of the liposomes triggered by the surfactant, Triton X. As shown in Figure 4a, the fluorescence signal of different vials of increasing concentration of NoV in the range of 10^2−10^5 copies mL^{-1} clearly shows the presence of increasing concentration of liberated calcein. The calibration line, calculated from the fluorescence intensities, is plotted in Figure 4b, which preserves the linearity over the wide concentration range with a correlation coefficient of 0.987. The limit of detection was calculated from the calibration line, which is 136 copies mL^{-1}.[44] As the method involves magnetic separation and thereafter liposomal amplification, it is expected to achieve good sensitivity even in real virus samples. In addition, the confocal images of calcein−liposome/virus/Fe_3O_4 nanoconjugates before (Figure 4c−f) and after Triton X treatment (Figure 4g,h) also confirm our hypothesis. The excellent color of calcein-filled liposomes is completely ruptured after the Triton X treatment, which indicates the successful release of the encapsulated calcein from the liposomes.

Selectivity and Stability of the Calcein−Liposome and Fe_3O_4 System. The interaction between the target virus with the calcein−liposome and the Fe_3O_4 nanoparticles is functioned by the monoclonal antibody conjugation. Therefore, it is obvious that the sensor should possess high specificity. However, to confirm any nonspecific interaction of the proposed sensor, the selectivity experiment was carried out in the presence of serum medium and other related viruses of the influenza virus (10^5 copies mL^{-1}), hepatitis E virus-like particle (10^{-9} g mL^{-1}), and zika virus (10^6 copies mL^{-1}). The bare buffer solution without any viruses and 10-fold diluted human serum samples were treated as the negative control to verify the matrix effect. The sensor in buffer and serum (as the negative control) did not show any significant signal as the sensing process involves the magnetic separation step (Figure 5a), which can effectively eliminate the interferences. However, in the case of the other interfering viruses, there was a very small signal observed, which may be due to some nonspecific interaction with the membrane of the liposomal matrix. Overall, the selectivity results prove that the fluorescence signal is observed only in the presence of the specific target virus.

https://dx.doi.org/10.1021/acsabm.0c00213
ACS Appl. Bio Mater. 2020, 3, 3560−3568

There is a possible disadvantage while using liposomes and antibody in any sensing work as these two suffer from stability issues when the sensor is treated for a long term.[45,46] Therefore, to observe the stability of the sensor during long-term use, NoV detection was performed repeatedly over a 1-month period. Although the individual components of calcein−liposome and the Fe_3O_4 nanoparticles were preserved at 4 °C, the liposome and the effectiveness of the antibody show obvious degradation over time, resulting in a noteworthy decline in performance within the first week of storage (Figure 5b). However, the sensor can show appreciable performance up to three weeks of storage. After that, due to the possible degradation of antibody and the poor stability of the liposome (shown in Figure S4), the background signal (without Triton X addition) makes the system less reliable and unable to use.

CONCLUSIONS

In this work, a liposome-based amplification system has been developed for the detection of the NoV, where a small number of virus particles can produce amplified intense signals. The theme of this work was schematically shown, where a new class of calcein-encapsulated liposomes and APTES-functionalized Fe_3O_4 nanoparticles was formulated. These two nanoparticles were functionalized with monoclonal NoV antibody to achieve specificity. Their mixture was used to form calcein−liposome/NoV/Fe_3O_4 nanoconjugates only in the presence of target NoV. A wide range of virus concentrations from 10^2 to 10^5 copies mL^{-1} has been used in the sensor to verify its applicability. Due to the presence of Fe_3O_4, the calcein−liposome/NoV/Fe_3O_4 nanoconjugates were separated from the analyte medium, eliminating the possible interferences, and then externally burst to release fluorophores from the core of the liposome. Therefore, a large number of fluorophores resulted from a small number of viruses and amplified the detection signal significantly, which reduced the detection limit as low as 136 copies mL^{-1}. Additionally, negligible cross-reactivity with similar viruses and other interferences, even in serum matrixes, confirmed the specific nature of the sensor with low background signal. Summarizing all of the above results, it can be expected that the sensing arrangement can have the potential for application in different virus sensing systems in the near future.

ASSOCIATED CONTENT

Supporting Information

The Supporting Information is available free of charge at https://pubs.acs.org/doi/10.1021/acsabm.0c00213.

ELISA to confirm the antibody−antigen binding, stability of liposomes, interaction between liposome and Fe_3O_4, and approximate estimation of liposome and Fe_3O_4 nanoparticle (PDF)

AUTHOR INFORMATION

Corresponding Author

Enoch Y. Park − *Laboratory of Biotechnology, Research Institute of Green Science and Technology and Laboratory of Biotechnology, Graduate School of Science and Technology, Shizuoka University, Shizuoka 422-8529, Japan;* orcid.org/0000-0002-7840-1424; Phone: +81-54-238-4887; Email: park.enoch@shizuoka.ac.jp

Authors

Ankan Dutta Chowdhury − *Laboratory of Biotechnology, Research Institute of Green Science and Technology, Shizuoka University, Shizuoka 422-8529, Japan*

Sabrina Sharmin − *Laboratory of Biotechnology, Research Institute of Green Science and Technology, Shizuoka University, Shizuoka 422-8529, Japan*

Fahmida Nasrin − *Laboratory of Biotechnology, Graduate School of Science and Technology, Shizuoka University, Shizuoka 422-8529, Japan*

Masahito Yamazaki − *Research Institute of Electronics, Shizuoka University, Shizuoka 422-8529, Japan;* orcid.org/0000-0002-5959-9914

Fuyuki Abe − *Department of Microbiology, Shizuoka Institute of Environment and Hygiene, Shizuoka 420-8637, Japan*

Tetsuro Suzuki − *Department of Infectious Diseases, Hamamatsu University School of Medicine, Hamamatsu 431-3192, Japan*

Complete contact information is available at: https://pubs.acs.org/10.1021/acsabm.0c00213

Author Contributions

#A.D.C. and S.S. contributed equally to this work.

Notes

The authors declare no competing financial interest.

ACKNOWLEDGMENTS

The authors thank Professor K. Morita of Institute of Tropical Medicine, Nagasaki University, for providing virus samples.

REFERENCES

(1) Yamanaka, K.; Saito, M.; Kondoh, K.; Hossain, M. M.; Koketsu, R.; Sasaki, T.; Nagatani, N.; Ikuta, K.; Tamiya, E. Rapid detection for primary screening of influenza A virus: microfluidic RT-PCR chip and electrochemical DNA sensor. *Analyst* **2011**, *136*, 2064−2068.

(2) Li, H.; Ren, J.; Liu, Y.; Wang, E. Application of DNA machine in amplified DNA detection. *Chem. Commun.* **2014**, *50*, 704−706.

(3) Ahmed, S. R.; Hossain, M. A.; Park, J. Y.; Kim, S.-H.; Lee, D.; Suzuki, T.; Lee, J.; Park, E. Y. Metal enhanced fluorescence on nanoporous gold leaf-based assay platform for virus detection. *Biosens. Bioelectron.* **2014**, *58*, 33−39.

(4) Chowdhury, A. D.; Takemura, K.; Li, T.-C.; Suzuki, T.; Park, E. Y. Electrical pulse-induced electrochemical biosensor for hepatitis E virus detection. *Nat. Commun.* **2019**, *10*, No. 3737.

(5) Dutta Chowdhury, A.; Ganganboina, A. B.; Nasrin, F.; Takemura, K.; Doong, R.-a.; Utomo, D. I. S.; Lee, J.; Khoris, I. M.; Park, E. Y. Femtomolar detection of dengue virus DNA with serotype identification ability. *Anal. Chem.* **2018**, *90*, 12464−12474.

(6) Chowdhury, A. D.; Park, E. Y. Detection of Infectious Viruses using Advanced Nanobiotechnology for Green Society. *Green Sci. Technol.* **2019**, 316−331.

(7) Ganganboina, A. B.; Dutta Chowdhury, A.; Doong, R.-a. N-doped graphene quantum dots-decorated V2O5 nanosheet for fluorescence turn off−on detection of cysteine. *ACS Appl. Mater. Interfaces* **2018**, *10*, 614−624.

(8) Ganganboina, A. B.; Doong, R.-a. Functionalized N-doped graphene quantum dots for electrochemical determination of cholesterol through host-guest inclusion. *Microchim. Acta* **2018**, *185*, No. 526.

(9) Huang, Y.; Tan, J.; Cui, L.; Zhou, Z.; Zhou, S.; Zhang, Z.; Zheng, R.; Xue, Y.; Zhang, M.; Li, S.; et al. Graphene and Au NPs co-mediated enzymatic silver deposition for the ultrasensitive electrochemical detection of cholesterol. *Biosens. Bioelectron.* **2018**, *102*, 560−567.

(10) Lai, Y.; Deng, Y.; Yang, G.; Li, S.; Zhang, C.; Liu, X. Molecular imprinting polymers electrochemical sensor based on AuNPs/PTh

modified GCE for highly sensitive detection of carcinomaembryonic antigen. *J. Biomed. Nanotechnol.* **2018**, *14*, 1688−1694.
(11) Lai, Y.; Wang, L.; Liu, Y.; Yang, G.; Tang, C.; Deng, Y.; Li, S. Immunosensors based on nanomaterials for detection of tumor markers. *J. Biomed. Nanotechnol.* **2018**, *14*, 44−65.
(12) Bui, M.-P. N.; Ahmed, S.; Abbas, A. Single-digit pathogen and attomolar detection with the naked eye using liposome-amplified plasmonic immunoassay. *Nano Lett.* **2015**, *15*, 6239−6246.
(13) Caliendo, A. M.; Gilbert, D. N.; Ginocchio, C. C.; Hanson, K. E.; May, L.; Quinn, T. C.; Tenover, F. C.; Alland, D.; Blaschke, A. J.; Bonomo, R. A.; et al. Better tests, better care: improved diagnostics for infectious diseases. *Clin. Infect. Dis.* **2013**, *57*, S139−S170.
(14) Song, D.; Park, B. Porcine epidemic diarrhoea virus: a comprehensive review of molecular epidemiology, diagnosis, and vaccines. *Virus Genes* **2012**, *44*, 167−175.
(15) Rodak, L.; Valíček, L.; Šmíd, B.; Nevorankova, Z. An ELISA optimized for porcine epidemic diarrhoea virus detection in faeces. *Vet. Microbiol.* **2005**, *105*, 9−17.
(16) Munch, M.; Nielsen, L. P.; Handberg, K.; Jørgensen, P. H. Detection and subtyping (H5 and H7) of avian type A influenza virus by reverse transcription-PCR and PCR-ELISA. *Arch. Virol.* **2001**, *146*, 87−97.
(17) Calvet, G.; Aguiar, R. S.; Melo, A. S.; Sampaio, S. A.; De Filippis, I.; Fabri, A.; Araujo, E. S.; de Sequeira, P. C.; de Mendonça, M. C.; de Oliveira, L.; et al. Detection and sequencing of Zika virus from amniotic fluid of fetuses with microcephaly in Brazil: a case study. *Lancet Infect. Dis.* **2016**, *16*, 653−660.
(18) Boonham, N.; Kreuze, J.; Winter, S.; van der Vlugt, R.; Bergervoet, J.; Tomlinson, J.; Mumford, R. Methods in virus diagnostics: from ELISA to next generation sequencing. *Virus Res.* **2014**, *186*, 20−31.
(19) Gavin, P. J.; Thomson, R. B., Jr Review of rapid diagnostic tests for influenza. *Clin. Appl. Immunol. Rev.* **2004**, *4*, 151−172.
(20) He, Z.; Tang, C.; Chen, X.; Liu, H.; Yang, G.; Xiao, Z.; Li, W.; Deng, Y.; Jin, L.; Chen, H.; et al. Based on magnetic beads to develop the kit for extraction of high-quality cell-free DNA from blood of breast cancer patients. *Mater. Express* **2019**, *9*, 956−961.
(21) Caygill, R. L.; Blair, G. E.; Millner, P. A. A review on viral biosensors to detect human pathogens. *Anal. Chim. Acta* **2010**, *681*, 8−15.
(22) Lum, J.; Wang, R.; Lassiter, K.; Srinivasan, B.; Abi-Ghanem, D.; Berghman, L.; Hargis, B.; Tung, S.; Lu, H.; Li, Y. Rapid detection of avian influenza H5N1 virus using impedance measurement of immuno-reaction coupled with RBC amplification. *Biosens. Bioelectron.* **2012**, *38*, 67−73.
(23) Zhang, G.-J.; Zhang, L.; Huang, M. J.; Luo, Z. H. H.; Tay, G. K. I.; Lim, E.-J. A.; Kang, T. G.; Chen, Y. Silicon nanowire biosensor for highly sensitive and rapid detection of Dengue virus. *Sens. Actuators, B* **2010**, *146*, 138−144.
(24) Liu, Q.; Boyd, B. J. Liposomes in biosensors. *Analyst* **2013**, *138*, 391−409.
(25) Chang, Y.-F.; Fu, C.; Chen, Y.-T.; Jou, A. F.-J.; Chen, C.-C.; Chou, C.; Ho, J.-a. A. Use of liposomal amplifiers in total internal reflection fluorescence fiber-optic biosensors for protein detection. *Biosens. Bioelectron.* **2016**, *77*, 1201−1207.
(26) Chowdhury, A. D.; Park, E. Y. Methylene blue-encapsulated liposomal biosensor for electrochemical detection of sphingomyelinase enzyme. *Sens. Actuators, B* **2019**, *301*, No. 127153.
(27) Alizadeh-Ghodsi, M.; Zavari-Nematabad, A.; Hamishehkar, H.; Akbarzadeh, A.; Mahmoudi-Badiki, T.; Zarghami, F.; Moghaddam, M. P.; Alipour, E.; Zarghami, N. Design and development of PCR-free highly sensitive electrochemical assay for detection of telomerase activity using Nano-based (liposomal) signal amplification platform. *Biosens. Bioelectron.* **2016**, *80*, 426−432.
(28) Akbarzadeh, A.; Rezaei-Sadabady, R.; Davaran, S.; Joo, S. W.; Zarghami, N.; Hanifehpour, Y.; Samiei, M.; Kouhi, M.; Nejati-Koshki, K. Liposome: classification, preparation, and applications. *Nanoscale Res. Lett.* **2013**, *8*, No. 102.
(29) Wehbe, M.; Malhotra, A.; Anantha, M.; Roosendaal, J.; Leung, A. W.; Plackett, D.; Edwards, K.; Gilabert-Oriol, R.; Bally, M. B. A simple passive equilibration method for loading carboplatin into pre-formed liposomes incubated with ethanol as a temperature dependent permeability enhancer. *J. Controlled Release* **2017**, *252*, 50−61.
(30) He, S.; He, L.; Liu, B.; Yu, S.; Tian, Y.; Wang, J.; Ding, L.; Wang, Y.; Qu, L.; Yu, F.; et al. Development of a rapid and sensitivity magnetic chemiluminescence immunoassay for DNA methyltransferase 1 in human serum. *Chin. Chem. Lett.* **2019**, *30*, 1031−1034.
(31) Mou, X.; Sheng, D.; Bao, Z.; Su, F.; Fan, X.; Zhu, Y.; Ye, K.; Zhou, Q.; Zhang, H.; Xu, C.; Liu, H. Correlation Between Genotypes and Allele Frequency of Lymphotoxin-Alpha and Gastric Cancer via Magnetic Separation Dual-Color Fluorescent Genotyping. *Nanosci. Nanotechnol. Lett.* **2019**, *11*, 1457−1463.
(32) Parker, T. D.; Kitamoto, N.; Tanaka, T.; Hutson, A. M.; Estes, M. K. Identification of genogroup I and genogroup II broadly reactive epitopes on the norovirus capsid. *J. Virol.* **2005**, *79*, 7402−7409.
(33) Ahmed, S. R.; Takemeura, K.; Li, T.-C.; Kitamoto, N.; Tanaka, T.; Suzuki, T.; Park, E. Y. Size-controlled preparation of peroxidase-like graphene-gold nanoparticle hybrids for the visible detection of norovirus-like particles. *Biosens. Bioelectron.* **2017**, *87*, 558−565.
(34) Ganganboina, A. B.; Chowdhury, A. D.; Khoris, I. M.; Nasrin, F.; Takemura, K.; Hara, T.; Abe, F.; Suzuki, T.; Park, E. Y. Dual modality sensor using liposome-based signal amplification technique for ultrasensitive norovirus detection. *Biosens. Bioelectron.* **2020**, *157*, No. 112169.
(35) Dutta Chowdhury, A.; Agnihotri, N.; Doong, R.-a.; De, A. Label-free and nondestructive separation technique for isolation of targeted DNA from DNA−protein mixture using magnetic Au−Fe_3O_4 nanoprobes. *Anal. Chem.* **2017**, *89*, 12244−12251.
(36) Ganganboina, A. B.; Dutta Chowdhury, A.; Doong, R.-a. New avenue for appendage of graphene quantum dots on halloysite nanotubes as anode materials for high performance supercapacitors. *ACS Sustainable Chem. Eng.* **2017**, *5*, 4930−4940.
(37) Sharmin, S.; Islam, M. Z.; Karal, M. A. S.; Alam Shibly, S. U.; Dohra, H.; Yamazaki, M. Effects of lipid composition on the entry of cell-penetrating peptide oligoarginine into single vesicles. *Biochemistry* **2016**, *55*, 4154−4165.
(38) Epstein, H.; Afergan, E.; Moise, T.; Richter, Y.; Rudich, Y.; Golomb, G. Number-concentration of nanoparticles in liposomal and polymeric multiparticulate preparations: empirical and calculation methods. *Biomaterials* **2006**, *27*, 651−659.
(39) Nasrin, F.; Chowdhury, A. D.; Takemura, K.; Lee, J.; Adegoke, O.; Deo, V. K.; Abe, F.; Suzuki, T.; Park, E. Y. Single-step detection of norovirus tuning localized surface plasmon resonance-induced optical signal between gold nanoparticles and quantum dots. *Biosens. Bioelectron.* **2018**, *122*, 16−24.
(40) Ku, A.; Chan, C.; Scollard, D.; Reilly, R. Chemical linkage of His6-containing peptides to Panitumumab antibody Fab fragments to enable labeling with 99mTc (I)-tricarbonyl complex. *J. Nucl. Med.* **2017**, *58*, 673.
(41) Kou, B.; Huang, W.; Neill, F. H.; Palzkill, T.; Estes, M. K.; Atmar, R. L. Norovirus antigen detection with a combination of monoclonal and single-chain antibodies. *J. Clin. Microbiol.* **2015**, *53*, 3916−3918.
(42) Hanson, M. C.; Abraham, W.; Crespo, M. P.; Chen, S. H.; Liu, H.; Szeto, G. L.; Kim, M.; Reinherz, E. L.; Irvine, D. J. Liposomal vaccines incorporating molecular adjuvants and intrastructural T-cell help promote the immunogenicity of HIV membrane-proximal external region peptides. *Vaccine* **2015**, *33*, 861−868.
(43) Suga, K.; Umakoshi, H. Detection of nanosized ordered domains in DOPC/DPPC and DOPC/Ch binary lipid mixture systems of large unilamellar vesicles using a TEMPO quenching method. *Langmuir* **2013**, *29*, 4830−4838.
(44) Dutta Chowdhury, A.; Doong, R.-a. Highly sensitive and selective detection of nanomolar ferric ions using dopamine functionalized graphene quantum dots. *ACS Appl. Mater. Interfaces* **2016**, *8*, 21002−21010.

https://dx.doi.org/10.1021/acsabm.0c00213
ACS Appl. Bio Mater. 2020, 3, 3560−3568

(45) Liu, D.; Huang, L. pH-sensitive, plasma-stable liposomes with relatively prolonged residence in circulation. *Biochim. Biophys. Acta, Biomembr.* **1990**, *1022*, 348−354.
(46) Thiagarajan, G.; Semple, A.; James, J. K.; Cheung, J. K.; Shameem, M. *A Comparison of Biophysical Characterization Techniques in Predicting Monoclonal Antibody Stability*; MAbs, Taylor & Francis, 2016; pp 1088−1097.

https://dx.doi.org/10.1021/acsabm.0c00213
ACS Appl. Bio Mater. 2020, 3, 3560−3568